The content, chemical state and accumulation of vanadium in a drill core of Alum shale from Kinnekulle

Niklas Gunnarsson

Dissertations in Chemistry at Lund University,
Bachelor's thesis
(15 hp/ECTS credits)

Department of Chemistry
Lund University
2019

The content, chemical state and accumulation of vanadium in a drill core of Alum shale from Kinnekulle

Bachelor's thesis

Niklas Gunnarsson

Department of Chemistry
Lund University
2019

Contents

Cover Picture: The Alum shale segment of the drill core from Kinnekulle.

The content, chemichal state and accumulation of vanadium in a drill core of Alum shale from Kinnekulle

Niklas Gunnarsson

Gunnarsson, N., 2019: The content, chemichal state and accumulation of vanadium in a drill core of Alum shale from Kinnekulle. *Dissertations in Chemistry at Lund University*, 15 hp (15 ECTS credits) .

Abstract: Exploitation of alum shale is a controversial subject in Sweden due to the history of pollution of the environment and groundwater, from past mining industries. The extraction of vanadium from alum shale is no different. Nevertheless the metal is a valuable resource used in tools, building, industries and aerospace materials. A look to the future reveals that vanadium may play a role in renewable energy. Vanadium redox flow batteries can store large amount of energy utilizing the many oxidation state of vanadium. This could solve the problem of energy storage many sources of renewable energy faces. This project is devoted to give a better understanding of how vanadium is bound and accumulated in the Cambrian Alum Shale Formation of southern Sweden, with the hope that this knowledge can help find an environmental friendly process to extract vanadium from alum shale in the future. In this project a drill core penetrating the Alum Shale Formation at Kinnekulle, has been analyzed with x -ray fluorescence spectroscopy, x-ray powder diffraction, x-ray photoelectron spectroscopy, IR-spectroscopy and a total organic carbon analysis. The aim is to identify the chemical state and evaluate possible correlations between vanadium, trace elements, organic carbon and minerals. The amount of vanadium increased towards the top of the drill core, but decreased at the top-most section. The drill core was found to be enriched in several trace elements, such as vanadium, barium, molybdenum, uranium, lead, copper and nickel, compared to Clarke values of black shale. Illite, the suspected main carrier of vanadium, had a very low signal in the x-ray powder diffraction and organic matter is proposed as a major carrier of vanadium. The level of anoxia in the waters at the time of sedimentation showed a rise in dissolved oxygen at 1,02 m., which could be the cause of the lower amount of vanadium in the top-most section of the drill core.

Keywords: Alum Shale Formation, Alum shale, Kinnekulle, Vanadium

Supervisors: Mikael Calner & Ola Wendt

Subject: Geochemistry

Niklas Gunnarsson, Department of Chemistry, Lund University, Naturvetarvägen 14, SE-223 62 Lund, Sweden. E-mail: ni0112gu-s@student.lu.se

Fig. 1. The Alum Shale Formation in the Kinnekulle drill core displayed. The lowermost part of the formation are at the top of the picture, where also 1,5 m of the underlying lower Cambrian sandstone can be seen. Simplified; the black areas are organic-rich black shale and the grey areas are bituminous limestone.

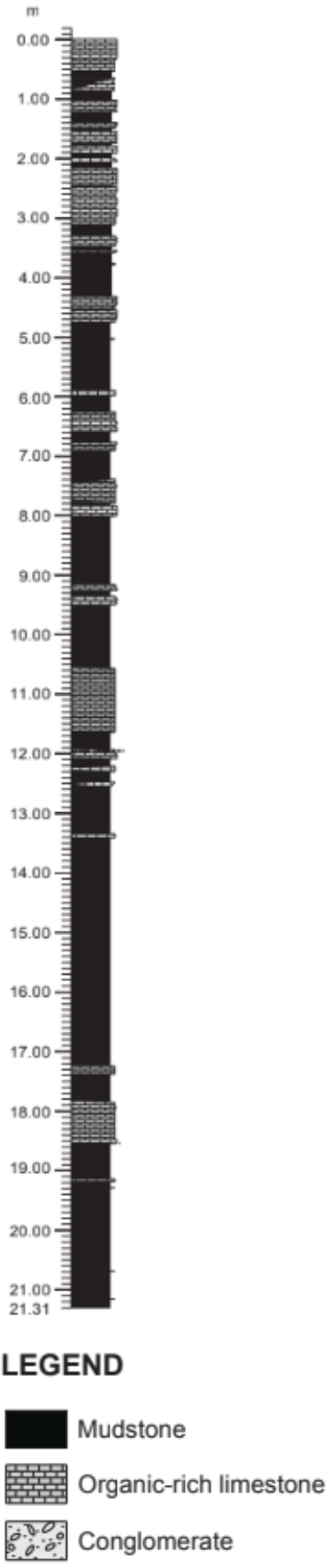

Fig. 2. A log of the Alum Shale Formation drill core showing mudstone, organic-rich limestone and conglomerates. Modified picture (from F. Lundberg, Department of Geology, LU).

1 Introduction

1.1 Vanadium

Vanadium is a silvery medium-hard transition metal which can be found in nature in many different oxidation states; (II), (III), (IV) and (V). The chemistry between the oxidation states is vast and vanadium often occur as oxoanions; vanadate in oxidations state (V) and vanadyl in oxidation state (IV). It is known to occur in about 150 minerals and is also dissolved in sea waters, rivers and lakes, often in form of vanadate in $H_2VO_4^-$. Vanadium is mainly used in alloys to produce specialized steel which even at high temperatures stays hard. Different alloys of vanadium, were it often plays a key role, can be found in aerospace materials, tools, buildings and pipelines etc. (Kelley et al. 2017).

A more recent use that may increase in the future, is in a new type of battery. Vanadium redox flow batteries utilizes all the above-mentioned oxidation states of vanadium to keep the charge in large tanks. The batteries can store large quantities of energy which could be useful for renewable energy. They are considered safer and sturdier and can even be fully discharged without any damage to the batteries (Energy Storage Association n.d.).

As the technology improves and use of the vanadium redox flow batteries might become more established, the demand for vanadium is likely to increase. Today vanadium is mainly produced as a byproduct in petroleum industries. The main suppliers are Russia, China and South Africa (Kelley et al. 2017). The cost of direct vanadium mining in black shales are at present often too steep both economically and environmentally. The batteries part in renewable energy contra the impact of vanadium mining on the environment is also an important assessment to be made in the future.

This project has investigated the vanadium in Alum Shale Formation, a type of black shale rich in organic carbon with wide distribution in Sweden, to give a better understanding of how it is distributed and bound in the rock. Perhaps this understanding could be useful in future enterprises to an easier and a more environmentally friendly mining of the metal.

1.2 The Kinnekulle drill core

The samples derive from a drill core, shown in *figure 1*, from Kinnekulle, Västergötland, (recovered 2016 M. Calner, Department of Geology, LU). Figure 2 depicts the log of the drill core (from F. Lundberg, Department of Geology, LU). Kinnekulle is a table mountain on the southern shore of Lake Vänern, which has been the target of several different mining enterprises who exploited the rocks since medieval times. The Alum Shale formation is ca 21 m thick in the drill core, and apart from black shale, also include bituminous limestone and conglomerates. The lowermost ca 10 meters of the formation belong to the Middle Cambrian whereas the upper ca 11 m are of Upper Cambrian (Furongian age). It is at this stage uncertain if the Ordovician part of the Alum Shale Formation is present in the core.

1.3 Alum Shale and Vanadium Accumulation

Alum shale is a type of sedimentary rock. Its distribution in the Fennoscandian part of the paleo continent Baltica, is geographically vast (Andersson et al. 1985). In Sweden it has a patch occurrence from Scania in the south, to Öland in the east and along the Scandinavian mountain range in Jämtland and Lappland to the north. The onset of black shale deposition varies in time between different areas. In the Oslo area and in Scania sedimentations starts in early mid-Cambrian, in Västergötland in mid-Cambrian and in nothern Öland in late-Cambrian (Buchardt et al. 1997). The formation is mostly made up of black shale, which is a black laminated rock with a high content of organic carbon and pyrite. It also contains bituminous limestone. The alum shale is distinguished by sedimentation in an anaerobic marine depositional, a unique biostratigraphy and a high content of organic carbon (Buchardt et al. 1997). The content of calcium carbonate is generally low and concentrated to the bituminous limestone. The shales have a high amount of trace metals (V, U, Mo, Ni, Co, Cr etc.) that vary in quantity depending on stratigraphic position within the formation (Andersson et al. 1985). The compositional variation of trace elements is also dependent on the different geochemical environments that shifted over time, including factors such as inflow of water and the amount of oxygen and sulfur present in the waters (Lerat et al. 2018).

Vanadium is found dissolved in water, which it may have entered due to chemical weathering and erosion of bedrock or through atmospheric deposition. The accumulation of vanadium into the sediments is dependent on several factors. First and foremost, there must be a steady supply of fluvial waters from which vanadium can accumulate and thereafter enter the sea floor sediments. For a significant amount of vanadium to accumulate, there must be a steady flow of water for a long period of time (Breit & Wanty 1991). This favors seawaters since it allows for continuous supply of the dissolved metal to the sediment. Vanadium mostly occurs in three different oxidation states, (III), (IV) and (V) and can be either anionic or cationic. Depending on the pH of the water, it reduces or oxidizes between the states. In most waters, where the pH is about 6-8.5, vanadium is present as vanadate (V) usually in the form of $H_2VO_4^-$. Vanadium readily undergo ligand chemistry and can be found in many different complexes, of which many are organic, dissolved in the waters. Complexes with vanadium (IV) will not be oxidized to vanadium (V) and therefore vanadium (IV) is also found in natural waters alongside vanadium (V) (Crans & Tracey 1998).

The accumulation of vanadium into the sediments is not fully understood, there are several pathways for vanadium to enter. One process is by adsorption to settling inorganic compounds, such as minerals that accumulate. In this process vanadate and vanadyl adorbs to iron(III)oxides (Shieh & Duedall 1988) and

aluminum oxides (Micera et al. 1988) which are deposited into the sediment.

Another way of accumulating vanadium is through living organisms. Vanadium is found in many various organisms. A possible entry into the food chain is through algae (Lee 1983) and plankton (Ünsal 1982). Expired organism and excretes of organisms are therefore a source of organically bound vanadium in the sediments. If the water is oxic, the accumulated Vanadium will dissolve before its more permanently bound (George N. Breit 1989). Anaerobic waters are also essential for organic matter to accumulate in the sediments (Lewan & Maynard 1982). In anoxic waters, vanadium (V) can be reduced by organic compounds or H_2S to vanadium (IV). This oxidative state is favored in adsorbing to organic particles (George N. Breit 1989). The binding to organic complexes gives a correlation between vanadium and organic carbon content.

A third process of accumulation vanadium is diffusion through the pores of the sediment where it can form complexes, with tetrapyrrole. This require organic matter previously deposited in the sediments. As an overlaying water provides a supply of vanadium and also nickel, the metals diffuse downwards to the pores of the sediment which has a lower concentration of vanadium due to its binding to complexes. The binding to tetrapyrroles and the supply of vanadium allow the diffusion to proceed. Tetrapyrroles is known to favorably bind bivalent cations generating an octahedral or square planar coordination. The bivalent cations which provides the most stable ligand energies is thus those of vanadium and nickel. The proportions in which vanadium and nickel binds to the complexes remains after diageneses. A large supply of tetrapyyroles preserved in the organic matter is also an essential factor (Lewan & Maynard 1982). The V / (Ni+V) ratio is a ratio used as a measurement of anoxia in the water, at the time of deposition. High value of this ratio indicates high level of anoxia. This allows sulfur to mobilize/reduce the vanadium, so it readily can bind to the complexes and hindering nickel as NiS_2 to bind. Oxic water would decrease the reduction of vanadium and the binding of NiS_2 while anoxic does not. The V / (Ni+V) does not increase lineary with sulfur content, but the sulfur needs to be enough to reduce the vanadium and bind the nickel (Wenger & Baker 1986).

The most common oxidative state of vanadium in black shale is (III) which is obtained by hydrogen sulfide as a reductant. Vanadium (III) remains stable in the clay during diagenesis to later be found in micas (George N. Breit 1989). It can also enter in several other minerals such as illite, metahewettite and patronite or even remain in organic matter if abundant (Kelley et al. 2017). Most micas transform to illite during diageneses due to high pressure and temperature. Illite has thus been found to be the main carrier of vanadium in black shale, where it has replaced aluminum after entering the crystal matrix and been reduced to vanadium (III) by organic matter. This can happen since vanadium (III) has a radius similar to Al (III) (Zhang et al. 2015).

Vanadium (IV) also occurs in clay minerals, adsorbed or in the matrix. It can also be found in organic compounds. Vanadium (V) can also be found, adsorbed to organic or inorganic particles in the black shale (Zhang et al. 2015). Pyrite is found to be the main metal bearing metal in alum shale, containing Mo, Cu, Ni, As, but small amounts of Pb, Zn and U. These can enter pyrite through ionic replacement, adsorption, precipitation or redox reactions (Lerat et al. 2018). Ni (II) has a radius close to Fe(II) and an octahedral coordination, same as pyrite, and can thus easily exchange for Fe(II) (Sternbeck et al. 2000) while As enters through exchange with S (Lerat et al. 2018). Pb and Zn enters through forming PbS or ZnS faster than FeS due to faster water exchange kinetics than Fe(II) (Morse & Luther 1999). Uranium adorbs to the surface of pyrite (Qafoku et al. 2009). Vanadium has only been found in pyrite to a lesser extent (Sternbeck et al. 2000).

1.4 Aim/Target

The aim of this project was to determine the variation of vanadium throughout the drill core and search for correlations with other elements or minerals. Another aim was to determine the oxidation state of the vanadium present and how it differs in different stratigraphic levels of the drill core. This was done with several different experimental techniques listed and described below under Methods.

2 Methods

2.1 Experimental Description

2.1.1 XRF-Spectroscopy (X-ray fluorescence)

XRF is a spectroscopy method used to determine the composition of materials. When the sample is irradiated with x-ray beams, the inner-shell electrons of the atoms is ejected creating a vacancy. Immediately afterwards, a relaxation occurs, an outer shell electron goes to the vacancy in the inner shell and emitting a photon with energy equal to the energy difference of the electron states. This process is called fluorescence. The x-ray fluorescence is measured by a detector. The energy of the emission is unique for every element and therefore the composition of the material can be determined. The lighter elements, sodium and those with lower atoms numbers, have too low fluorescence energy to be distinguished from the noise of the measurement (Kalnicky & Singhvi 2001).

2.1.2 XRD (Powder x-ray diffraction)

Solid materials with atoms arranged in orderly structure forming crystal lattices are known as crystals. Minerals have a crystal structure which can be detected using X-ray diffraction. If an x-ray irradiates a crystal, the x-rays are diffracted at the lattice planes because the length between the lattice planes matches

the length of the x-ray wavelength. The second reflected wavelength is a multiple of the first and this pattern goes on through the crystal lattice. The angles between the incoming x-ray and the diffracted light is the diffraction angle. This leads up to Bragg's equation which is used to determine diffraction patterns.

$$2dsin\theta = n\lambda \qquad \text{Bragg's equation}$$

The diffraction angle is 2θ, the spaces between the lattice planes is d and the wavelength of the x-ray is λ. In powder x-ray diffraction the sample is in a fine powder, allowing the crystals to orient randomly. The diffraction angles and their intensities are measured. The random scattering of crystals allows for powder patterns to be found which can be compared to data to determine crystal structures and identify e.g. minerals (Housecroft & Sharpe 2018).

2.1.3 XPS (X-ray photoelectron spectroscopy)

X-ray photoelectron spectroscopy is a method used to analyze the surfaces of materials, often metals. X-rays penetrate the sample with about 1 nm, giving the electron configuration and ionization energy of the atoms at the surface. The single wavelength x-ray beam ejects an electron from the inner shell, this process is called the photoelectric effect. For the electron to be ejected the energy of the photon must be more or equal to the binding energy of the electron. The ejected electron has a specific energy based on its electronic state. The energy of the incoming x-ray is equal to the electrons ionization energy plus the excess energy. Therefore the excess energy is measured which through a formula allows for the ionization energy to be determined and the element to be determined since the binding energy is unique.

$$KE = E_{ex} - IE$$

Kinetic energy is KE, the excess energy of the ejected electron. E_{ex} is the energy of the single wave length x-ray beam and IE is the ionization energy (Housecroft & Sharpe 2018). The ionization energy translate to binding energy since this is what was required to separate the electron from the nucleus. Since atoms of different oxidation state has different ionization energy, the oxidation state can also be determined. The spectra generated shows peaks of binding energy at the x-axis, with different intensities at the y-axis.

XPS is performed in an ultra-high vacuum to allow a free path for the beam without any gas molecule scattering the beam.

2.1.4 IR-Spectroscopy

IR (infrared)-spectroscopy is mainly used for qualitative determination of compounds which can be detected in the infrared spectra. Molecules vibrates at different frequencies. A molecule irradiated with light, absorb light of matching frequencies to their vibrations. Functional groups and molecules have unique vibrating frequencies, allowing them to be identified in a spectrum.

2.1.5 TOC-analysis (Total organic carbon)

TOC is an abbreviation for total organic carbon. To measure the organic carbon in a sample the inorganic carbon of an aliquot is first removed by acidification. Combustion is then used to convert the solid carbon to CO_2, which can be measured by a thermal conductivity detector. Both the acid treated aliquot and the untreated sample is measured and compared to conclude the amount of organic carbon.

2.2 Experimental Procedures

2.2.1 XRF-Spectroscopy

Between 1-21.31 meters in the drill core was measured about every 40 cm. The first 0–1 meters the measurements were done in much closer intervals. The beds of limestone made the intervals uneven in some cases. Discs from the drill core were lifted and had their surfaces washed to avoid contaminated readings. Then they were put upended on the portable XRF, which was mounted on a stationary platform. Each sample analysis was run one time, for four minutes.

The instrument used was made by ThermoFischer Scientific and the model was Niton XL3t GOLDD+ with a silver anode. It can detect elements from magnesium to uranium (ThermoFischer Scientific n.d.). An additional calibration was performed before the analysis with a standard of known composition.

2.2.2 XRD

A few samples were cut off from the drill core and grinded to a very fine powder. The powder was evenly distributed on a tape attached to a tray. The spectra were refined in the software Jana2006 and compared with crystalline data from vanadium bearing minerals with various likelihood of being present.

2.2.3 XPS

Samples that fit the required measurements of 10 x 10 x 5 mm were cut off the drill core. A first test was made to make sure it would be possible to acquire a spectrum, since the rock sample was not the typical sample type of conductive metals. The untreated sample was on a tray with copper tape and depressurized to about 10^-7 Pascal.

The next sample was cleaned in an ultrasonic bath three times using acetone, ethanol and distilled water as solvents. This was done in order to reduce noise and the peaks of carbon and oxygen to make vanadium peaks more visible.

The samples chosen for these measurement were the ones containing the most vanadium in order to have the greatest chance of detection.

2.2.4 IR-Spectroscopy

Eight samples were grinded to a powder. The

respective powders were then attached to the instrument as a pellet. The instrument had a region of 400-4000 cm^{-1}. The spectra was then compared with data of different vanadyl compounds.

2.2.5 TOC-analysis

Five samples were grinded to a powder. An aliquot of each sample was treated with 2 M HCl overnight in glass vials. The vials were centrifuged and decanted. The vials were then filled up with distilled water, centrifuged and decanted six times each to remove the acid. The samples were dried in the oven at 60 °C for about 65 hours. Small amount of each sample, treated and untreated, were weighed in tin capsules before the carbon levels were measured by combustion.

3 Results

3.1 XRF-Spectroscopy

The amount of vanadium in all 56 measured positions are presented in *table 1*.

The mean value of all the 56 measurements for each detected element and their median are presented in *table 2*, to get an overview of the bulk composition in the drill core. It should be noted that Co, Bi and W were not found throughout the drill core but concentrated in certain depth. Co was found at a depth of 18,96 m, Bi was found at 0,78 m depth, W was found at 2,48 m and 0,78 m depth and P was found at 20,89 m, 6,91 m, 4,86 m, 2,48 m, 1,76 m, 1,02 m, 0,83 m, 0,78 m and 0,56 m depth. The elements marked with an asterisk were pre-calibrated to be detectable by the manufacturer but were not part of the standard used for calibration before the analysis, these values have a higher degree of uncertainty. The calibration of P had a calibration error of a factor of 4,72 which is not adjusted for, value of P is highly uncertain.

All of the values in *table 2* were compared to Clarke values of black shales, which are compiled values of trace elements worldwide. The compilation are median values with standard deviations added to avoid influence of anomalies (Ketris & Yudovich 2009). The values were mostly similar in comparison. The highest positive deviations are shown in *table 3*. Most notable are Mo and U, which the drill core was enriched with 749 % and 704 % more than the average black shale. It should be noted that Mo was not in the calibration and thus has higher degree of uncertainty. Vanadium was found to be 137 % more than the average black shale. La and Ce which the instrument was calibrated for, has Clarke values of 28 ppm and 58 ppm respectively but was not found in the drill core. The instrument is pre-calibrated for and should detect Cl even though not calibrated for. Cl has a Clarke value of 300 ppm and was not detected.

The major elements of the drill core are Si, S, Al, Fe and K. Elements with a percentage above 0,5 % of the total composition are listed in *table 4*

Table 1: The amount of vanadium in ppm, and the standard deviation, at different depths.

Depth (m)	Vanadium (ppm)	2σ
0,56	503	33,9
0,62	588	34,9
0,74	519	28,5
0,78	367	32,8
0,83	269	27,2
0,86	301	29,8
0,93	367	33,2
0,98	336	33,2
1,02	279	34,6
1,33	522	33,0
1,76	755	43,1
2,09	519	34,1
2,48	633	55,4
3,15	577	50,0
3,50	637	45,6
3,88	614	43,7
4,23	1010	55,4
4,86	663	39,3
5,24	696	38,2
5,63	709	38,5
6,04	801	39,5
6,61	479	37,0
6,91	633	42,0
7,29	508	37,5
7,81	527	37,4
8,06	535	34,8
8,45	468	35,0
8,88	524	35,0
9,31	495	32,6
9,65	473	31,4
9,95	507	32,9
10,49	427	35,2
11,73	316	27,8
12,13	291	32,3
12,54	284	32,6
12,95	278	35,9
13,34	330	37,4
13,75	347	36,3
14,14	330	37,2
14,54	364	36,0
14,94	315	35,8
15,34	549	40,7
15,74	445	38,6
16,10	462	40,0
16,53	643	40,8
16,94	645	41,5
17,34	791	41,0
17,74	513	41,1
18,58	389	40,7
18,96	226	42,5
19,27	192	33,6
19,65	209	33,0
20,07	997	42,1
20,41	402	39,7
20,89	312	35,1
21,26	289	38,2

*Table 2: Elements, the mean value of their composition from the 56 measurements and the median. *Not in the calibration. **Not adjusted due to high error factor in calibration*

Element	Mean of bulk (ppm)	2σ	Median (ppm)
Ba	1160	26,5	889
Sn*	0,402	11,6	0
Mo*	176	3,65	170
Nb*	8,15	1,71	7,73
Th	5,25	4,87	0
Zr	172	3,40	162
Y*	37,9	1,85	23,8
Sr	219	4,03	178
U	65,9	3,11	68,4
Rb	172	1,84	155
Bi*	0,57	12,5	0
As	63,6	5,94	61,6
Pb	80,4	3,86	46,7
W*	2,04	40,3	0
Zn	52,6	7,58	49,6
Cu	132	12,7	134
Ni	202	12,7	191
Co*	2,24	109	0
Fe	29000	334	27800
Mn	236	42,7	194
Cr	94,1	24,9	93,6
V	485	37,4	487
Ti	2310	74,2	2190
Ca	7970	298	4600
K	22100	316	22200
Al	47400	1180	42700
P**	721	272	0
Si	160000	1020	157000
S*	70300	408	72800
Mg	7910	2310	8240

*Table 3: The elements with the highest positive deviation from Clarke values and their medians compared to the Clarke values and the deviation in percent. *Not in calibration.*

Element	Median (ppm)	Clarke (ppm)	Deviation (%)
Ba	889	500	77,8
Mo	170	20	750
U	68,4	8,5	705
As	61,6	30	105
Pb	46,7	21	122
Cu	134	70	91,2
Ni	191	70	173
V	487	205	138

Table 4: The major elements of the drill core and their percentage of the composition.

Elements	Mean of bulk (%)
Si	34,8
S	15,3
Al	10,3
Fe	6,31
K	4,80
Ca	1,73
Ti	0,502

A graphic representation of values in *table 4,* without standard deviations, can be seen in *figure 3*. The values are seen fluctuating with two peaks at around 1000 pm at 4,23 m and 20,07 m depths.

Graphic representations of the two elements with the highest deviations, U and Mo, from Clarke values can be seen in *figure 4 and 5*. Uranium has somewhat fluctuating value at first and consistent values between 12,13 - 21,26 m depth. Molybdenum is fluctuating a lot more than uranium. They both have a peak at 0,78 m.

A graphic representation of Ba have also been singles out and can be seen in *figure 6*. The values are somewhat consistent except at a depth of 2,48 – 4,23 m, which has greatly increased values.

The values of V and Ni are compared in *figure 7*. In the graph there seem to be a correlation in their increases and decreases between different measurements with the exception at a depth of 1,02 m where the amount of Ni suddenly increases but not V.

The ratio of V / (Ni + V) at different depth is presented in *figure 8*. The ratio is somewhat consistently concentrated in the area between 0,6 - 0,8 with an exception at 1,02 m depth which has a ratio of 0,43.

In *figure 9*, a graph can be seen with S and Fe which are the components of pyrite. A correlation is seen even though not perfect since there is deviation from the trend in some measurement point.

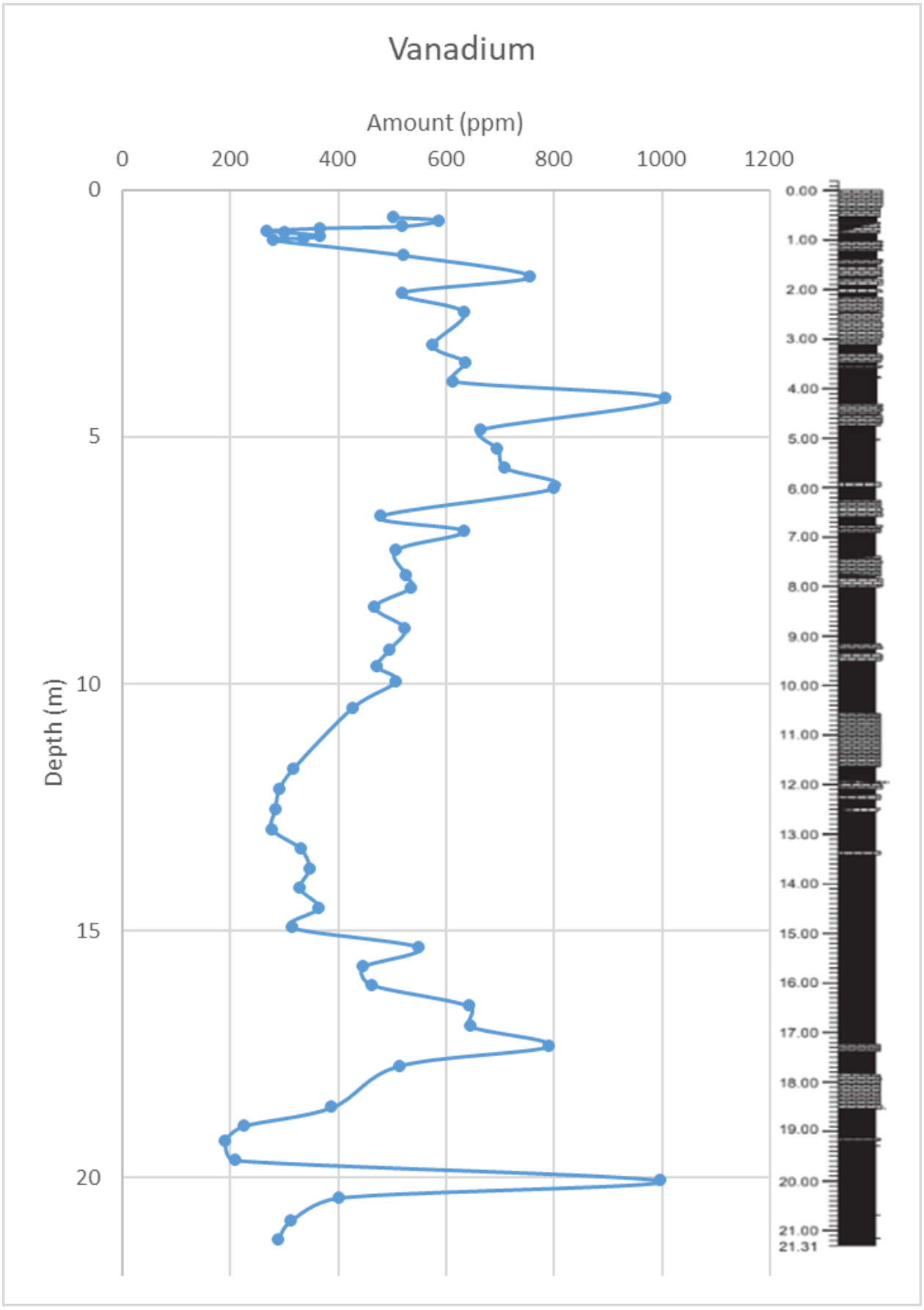

Fig. 3 The amount of vanadium in ppm, at different depths in the core section. The amount of vanadium is fluctuating with two peaks at around 1000 ppm at 4,23 m and 20,07 m depths respectively.

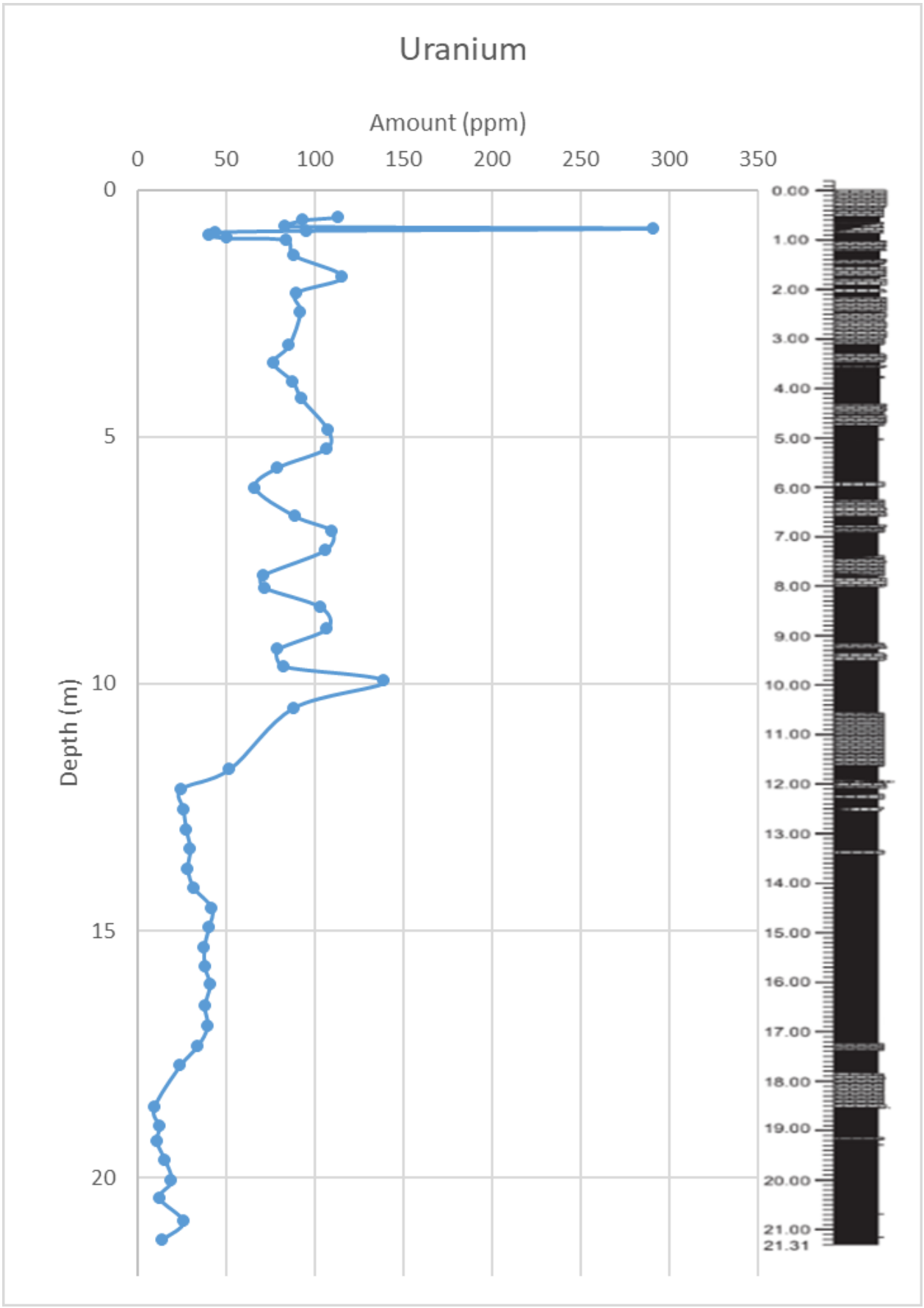

Fig. 4 The amount of uranium in ppm, at different depths in the core section. The value is consistently between 10 – 40 ppm between 12,13 – 21,26 m depth. The values is fluctuating from 0,56 – 11,73 m depth with a peak at 0,78 m.

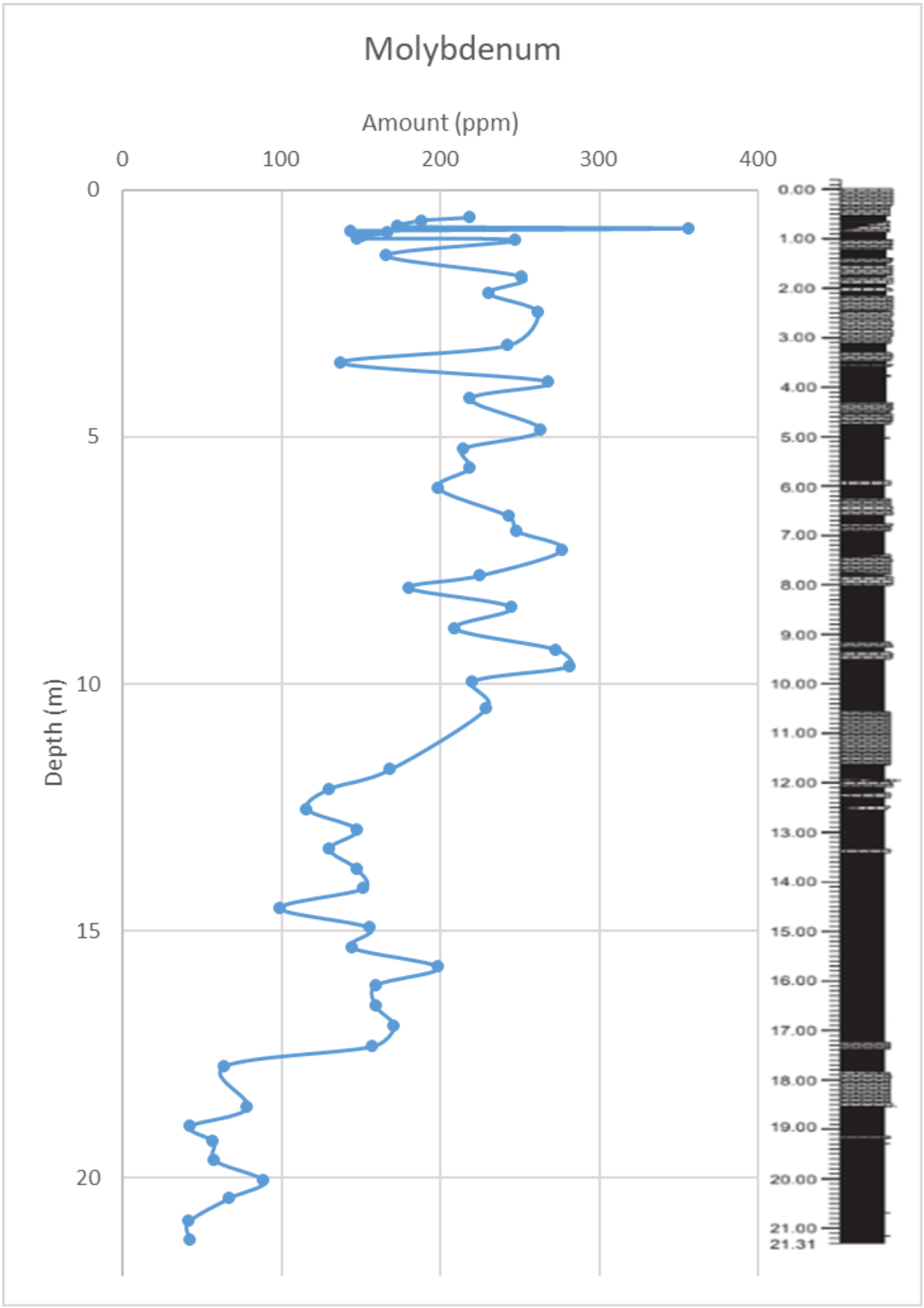

Fig. 5 The amount of molybdenum in ppm, at different depths in the core section. The amount is fluctuating and slowly rising from 21 to 0 m depth with a sudden 356 ppm peak at 0,78 m.

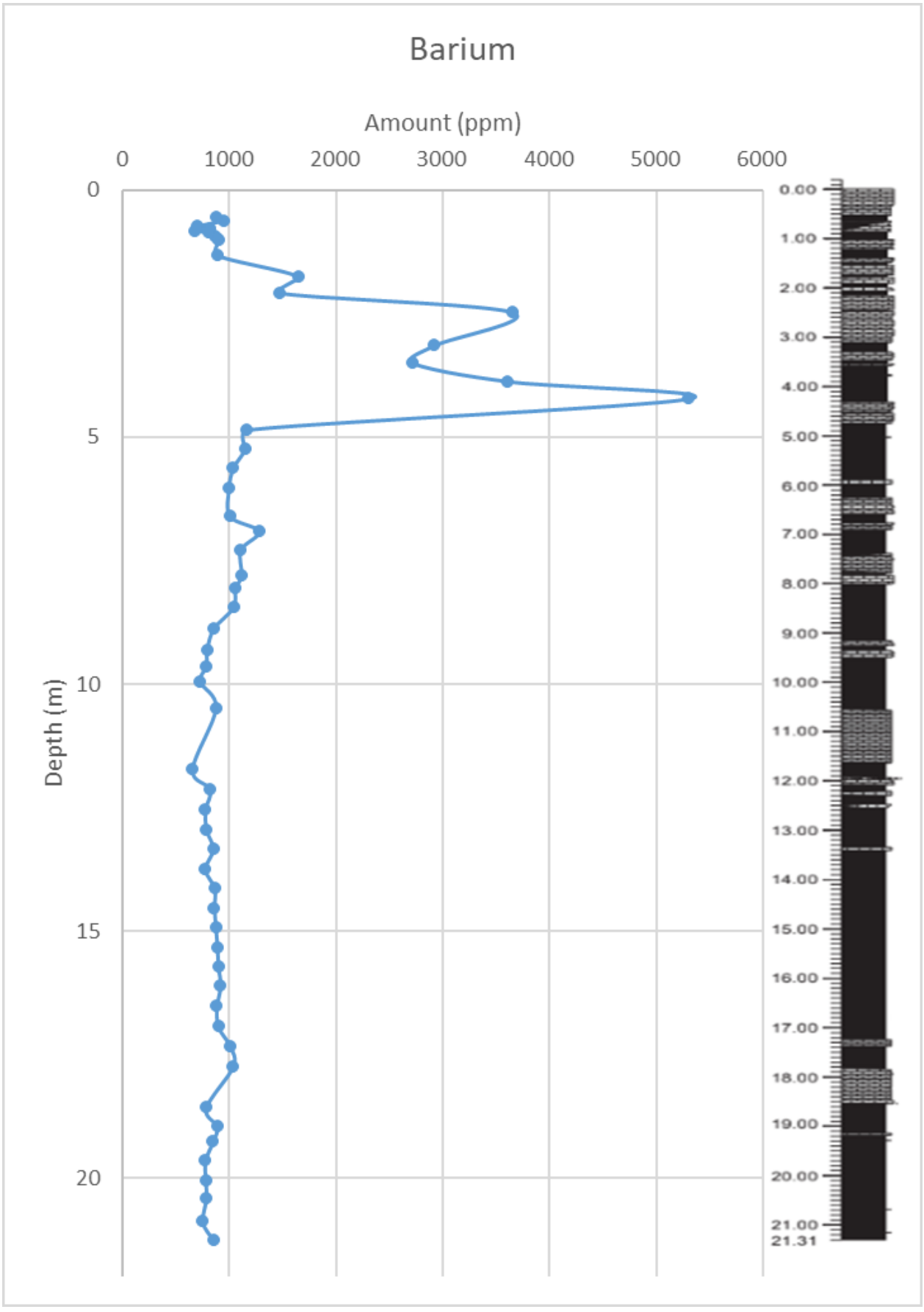

Fig. 6 The amount of barium in ppm, at different depths in the core section. The amount is consistently 700 – 1200 ppm from 21,26 – 4,86 m depth. There is a sudden increase at 423 m and a less sudden decline thereafter.

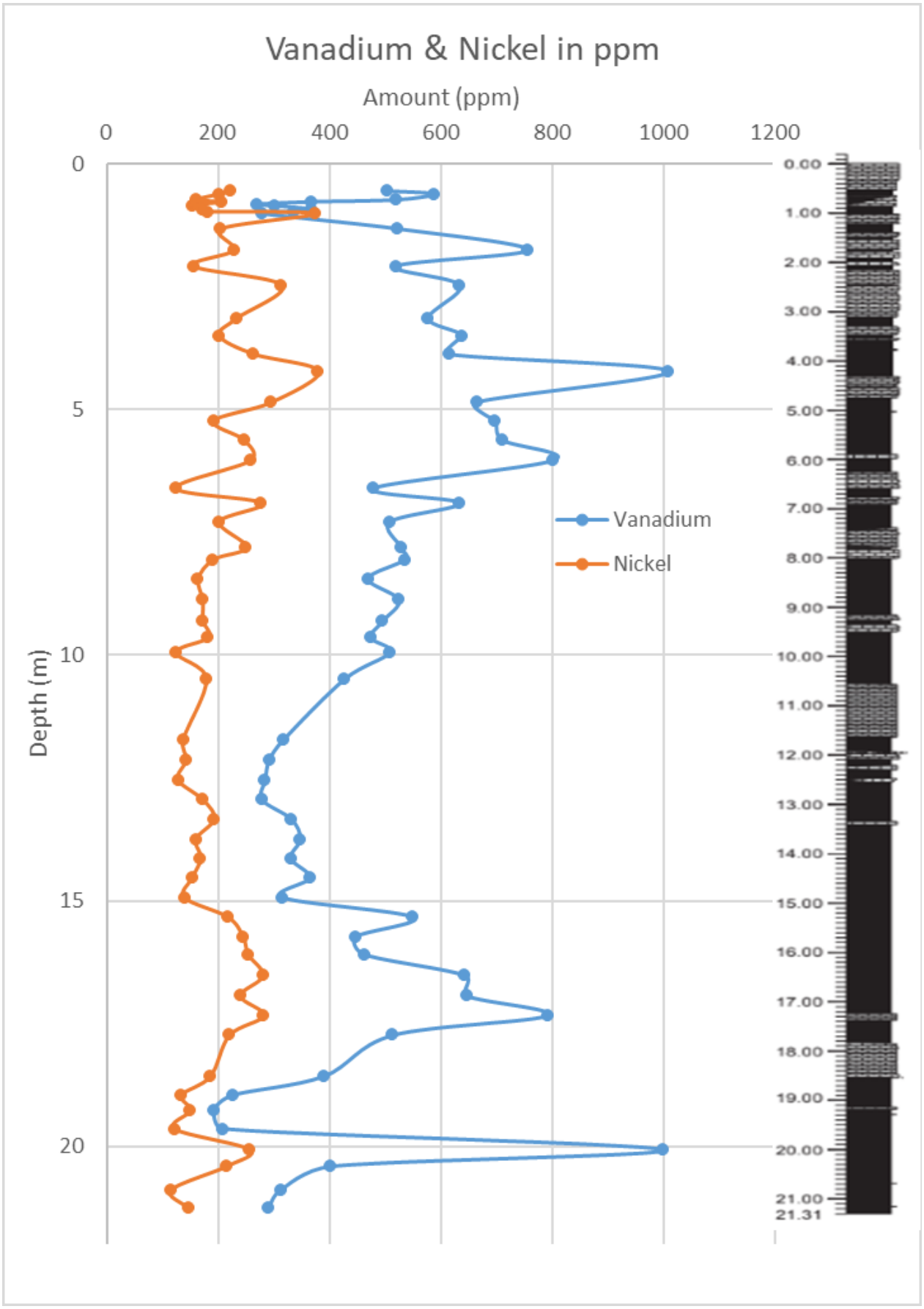

Fig. 7 The amount of vanadium and nickel in ppm with fluctuating values, at different depths in the core section.

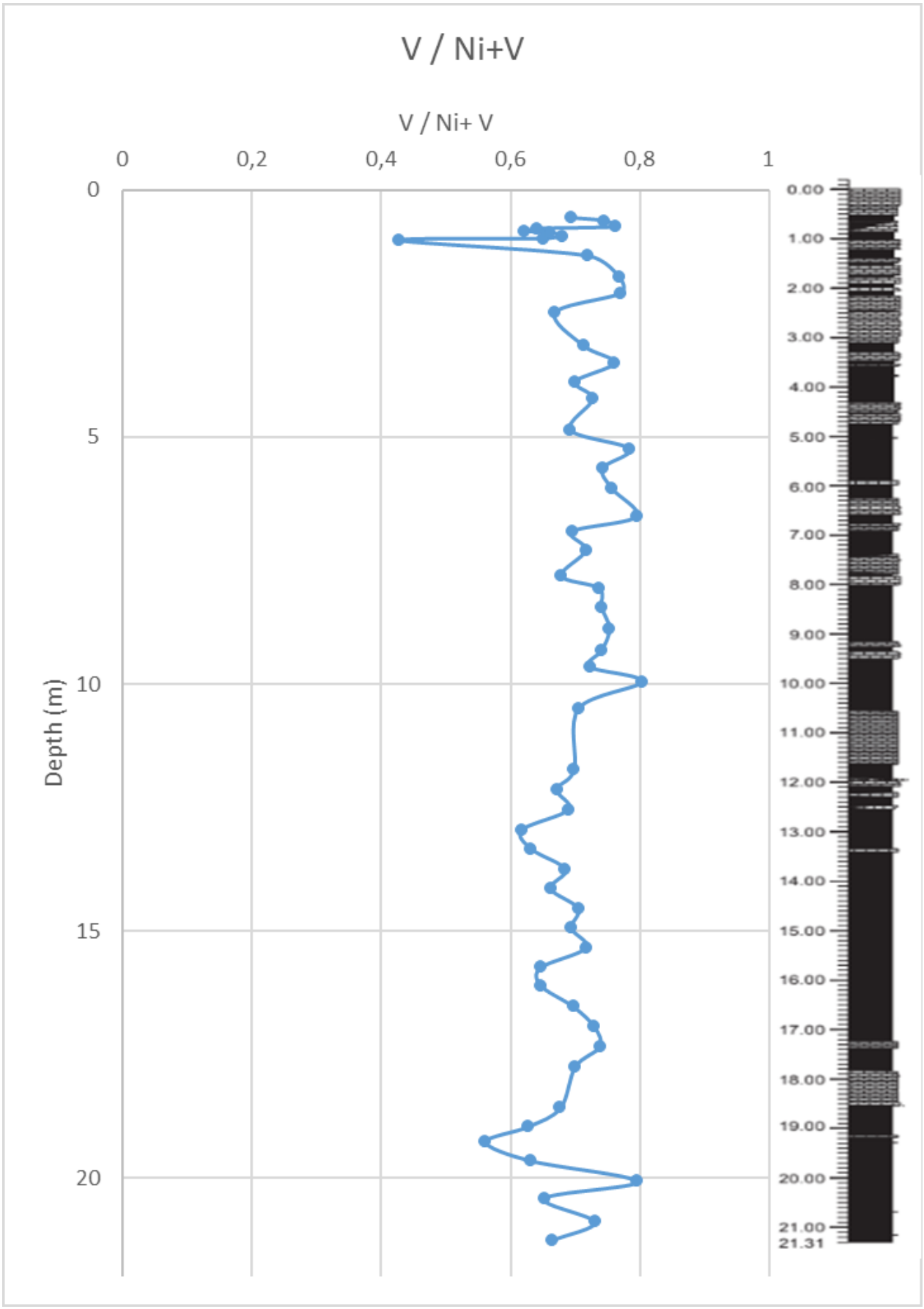

Fig. 8 The ratio of V / (Ni + V), at different depths in the core section. The ratio is consistently around 0,6 – 0,8 with the exception of 0,43 at 1,02 m depth.

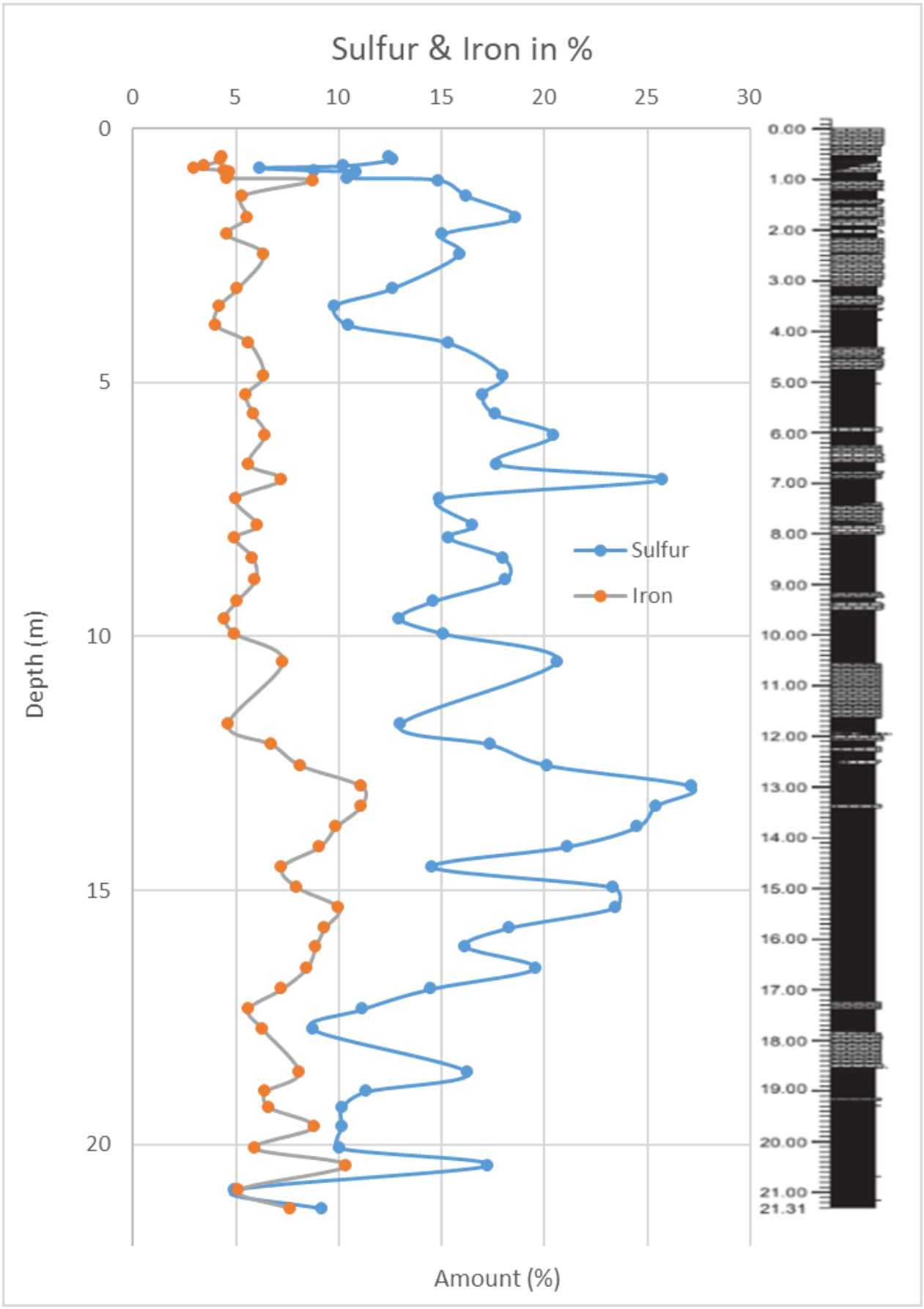

Fig. 9 The amount of sulfur and iron in percent with fluctuating values, at different depths.

3.2 XRD

Three samples were analyzed by x-ray powder diffraction. They were chosen for their variety in amount of vanadium and depth.

Table 5: The samples analyzed by x-ray powder diffraction.

Sample nr.	Vanadium (ppm)	Depth (m)
4	997	20,07
21	278	12,95
55	588	0,62

The spectra of sample 4 is depicted in *figure 10,* sample 21 in *figure 11* and sample 55 in *figure 12,* with 2θ at the x-axis and relative intensity at the y-axis. Almost all peaks were identified. Quartz was the most predominant mineral identified. Pyrite was the second most predominant. Illite has its three strongest peak at 2θ =20,03 (100% intensity), 2θ =35,02 (85% intensity) and 2θ=24,30 (40% intensity) according to data (Web mineral n.d.). Only the two strongest peak are occurring in the spectra. The spectrum of sample 21, in *figure 11*, shows stronger pyrite peaks than the other spectra.

The illite peaks of sample 4 are presented in *table 6,* sample 21 in *table 7* and sample 55 in *table 8*. $2\theta_{cal}$ and d_{cal} are calculated values from the software Jana2006. $2\theta_{obs}$ and d_{obs} are observed values from the spectrum. $2\theta_{diff}$ and d_{diff} are the difference in absolute values between calculated and observed values. Relative intensities and hkl-index are also presented. The second strongest observed peak in the spectrum is a mix of three peaks, all contributing.

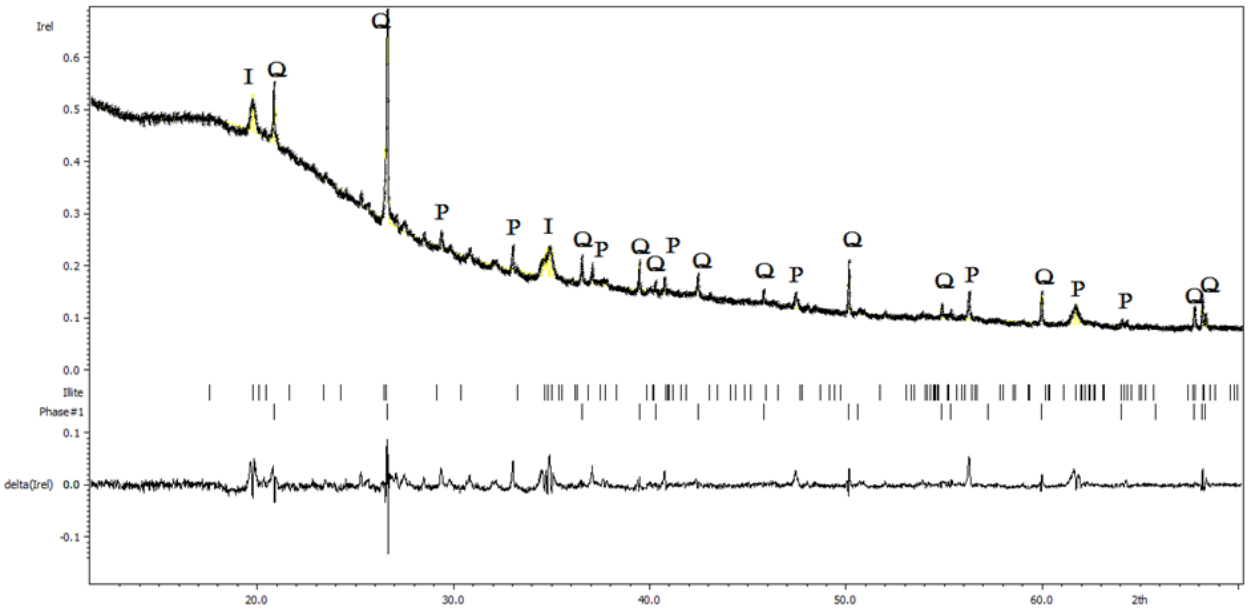

Fig. 10 The spectrum of sample 4 with relative intensity on the y-axis and the 2θ angle at the x-axis. The identified peaks has been marked with I for illite, Q for quartz and P for pyrite. In the middle the calculated 2θ angles has been marked for illite and quartz respectively. In the bottom of the graph the difference in relative intensities are shown.

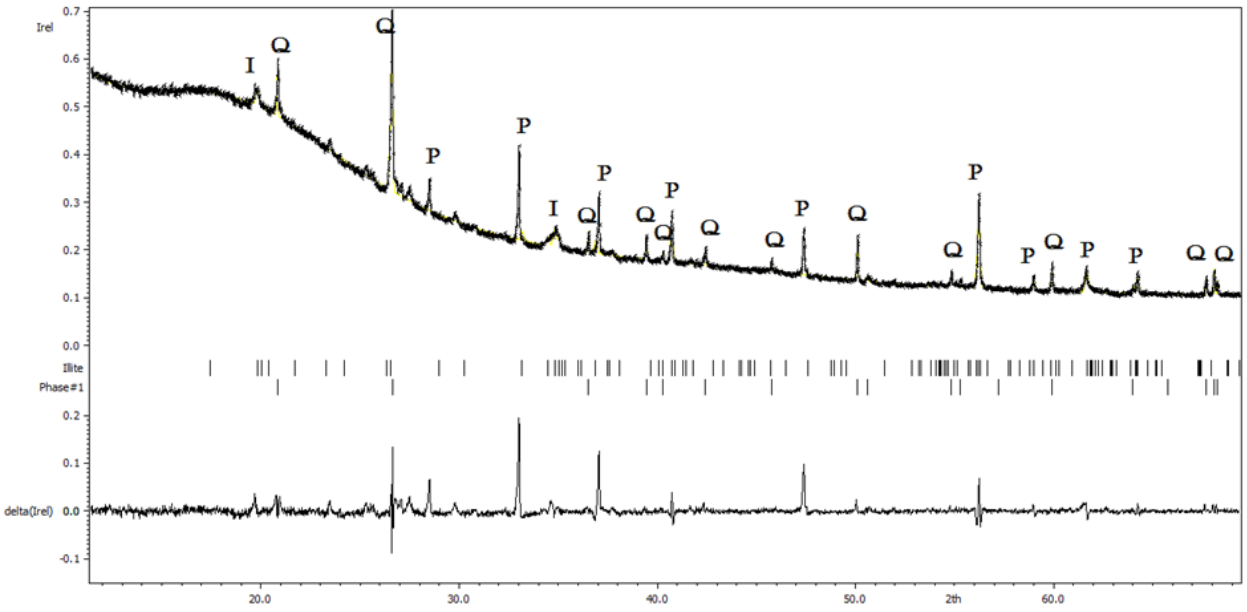

Fig. 11 The spectrum of sample 21 with relative intensity on the y-axis and the 2θ angle at the x-axis. The identified peaks has been marked with I for illite, Q for quartz and P for pyrite. In the middle the calculated 2θ angles has been marked for illite and quartz respectively. In the bottom of the graph the difference in relative intensities are shown.

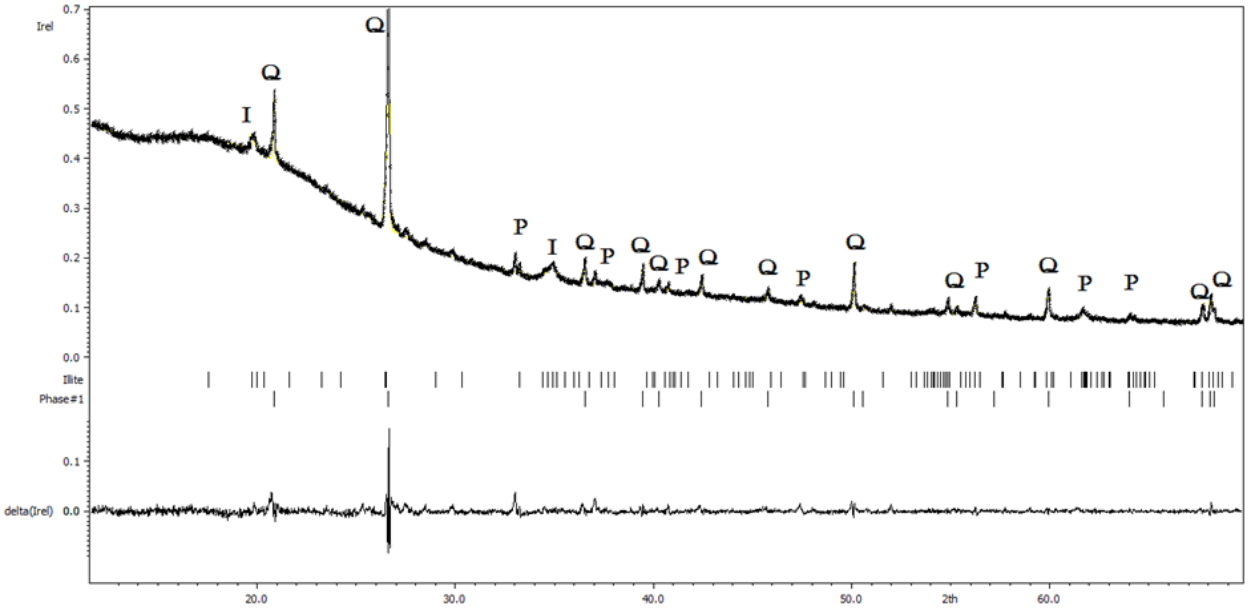

Fig. 12 The spectrum of sample 55 with relative intensity on the y-axis and the 2θ angle at the x-axis. The identified peaks has been marked with I for illite, Q for quartz and P for pyrite. In the middle the calculated 2θ angles has been marked for illite and quartz respectively. In the bottom of the graph the difference in relative intensities are shown.

Table 6: Diffraction values presented for sample 4; the calculated angles and d-spacing from Jana2006, 2θcal, and dcal, the observed *angle and d-spacing, 2θobs and dobs, the difference between observed and calculated values in absolute, the relative intensity and the hkl-index.*

2θcal	dcal (Å)	2θobs	dobs (Å)	2θdif	ddif (Å)	Relative intensity (%)	h	k	l
19,7566	4,4901	19,732	4,4956	0,0246	0,0055	51,88	0	2	0
34,4896	2,5984	34,477	2,5993	0,0126	0,0009	21,1	-2	0	1
34,7353	2,5803	34,721	2,5816	0,0143	0,0013	21,98	1	3	0
34,9529	2,565	34,888	2,5696	0,0649	0,0046	23,66	-1	3	1

Table 7: Diffraction values presented for sample 21; the calculated angles and d-spacing from Jana2006, 2θcal, and dcal, the observed angle and d-spacing, 2θobs and dobs, the difference between observed and calculated values in absolute, the relative intensity and the hkl-index.

2θcal	dcal (Å)	2θobs	dobs (Å)	2θdif	ddif (Å)	Relative intensity (%)	h	k	l
19,8397	4,4715	19,826	4,4745	0,0137	0,003	54,12	0	2	0
34,4666	2,6001	34,534	2,5951	0,0674	0,005	22,66	-2	0	1
34,8408	2,573	34,869	2,571	0,0282	0,002	24,84	1	3	0
35,0513	2,558	35,063	2,5572	0,0117	0,0008	22,37	-1	3	1

Table 8: Diffraction values presented for sample 55; the calculated angles and d-spacing from Jana2006, 2θcal, and dcal, the observed angle and d-spacing, 2θobs and dobs, the difference between observed and calculated values in absolute, the relative intensity and the hkl-index.

2θcal	dcal (Å)	2θobs	dobs (Å)	2θdif	ddif (Å)	Relative intensity (%)	h	k	l
19,7309	4,4959	19,764	4,4884	0,0331	0,0075	44,85	0	2	0
34,3875	2,6059	34,466	2,6001	0,0785	0,0058	17,73	-2	0	1
34,6741	2,585	34,764	2,5785	0,0899	0,0065	18,5	1	3	0
34,8959	2,569	34,931	2,5665	0,0351	0,0025	19,11	-1	3	1

3.3 XPS

The samples with the most vanadium were chosen to increase the chances of detection, these were nr. 4 (997 ppm) and nr. 40 (1010 ppm), presented in *table 1*.

Table 9: The samples analyzed by XPS.

Sample nr.	Vanadium (ppm)	Depth (m)
4	997	20,07
40	1010	4,23

The first analysis with sample nr. 4 a spectrum was obtained but vanadium peaks were too low to analyze. The second analysis with sample nr. 40 did not show any improvement even after ultra-sonication. No further tests were made.

3.4 IR-Spectroscopy

Eight samples, presented in *table 10*, were analyzed by IR-spectroscopy.

Table 10: The samples analyzed by IR-spectroscopy.

Sample nr.	Vanadium (ppm)	Depth (m)
4	997	20,07
5	209	19,65
10	791	17,34
17	364	14,54
21	278	12,95
36	801	6,04
40	1010	4,23
55	588	0,62

All spectra, except sample 5, were identical with some small variance in intensity and wavenumber. The spectrum of sample 21 is shown in *figure 13*.

The spectrum for sample 5 had an additional peak at 1436 cm^{-1} which was small and broad, shown in *figure 14*. All other spectra lacked this peak.

The objective to find a match for vanadyl, was not reached.

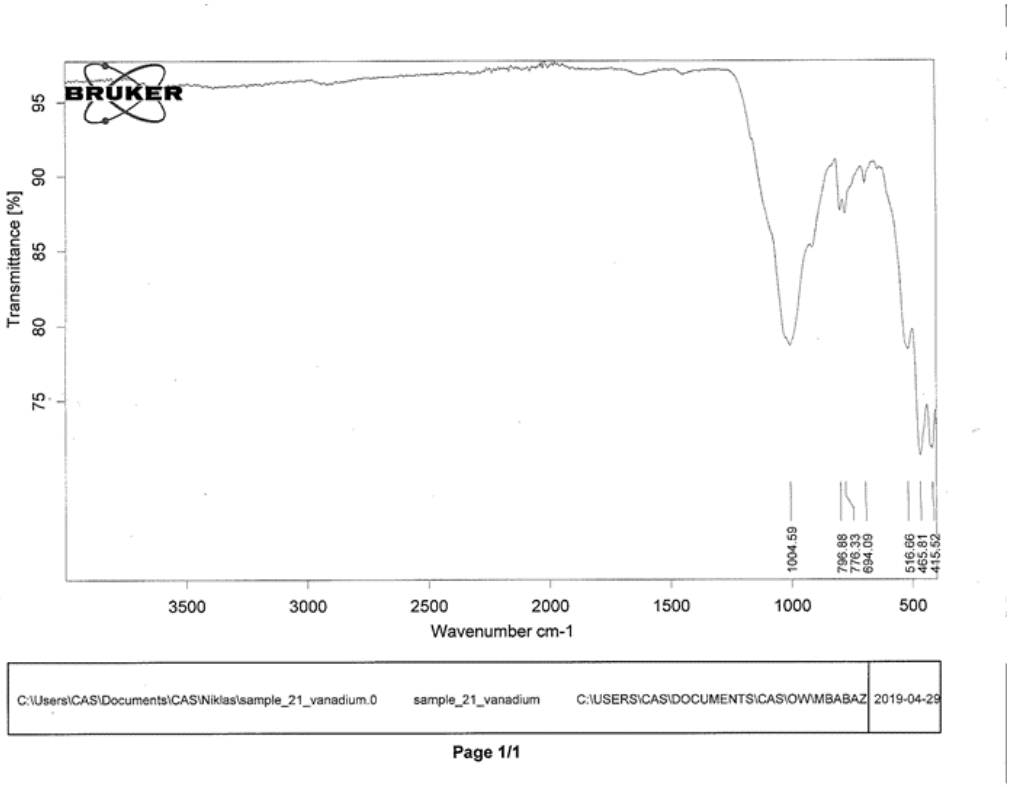

Fig. 13 Spectrum of sample 21. Transmittance (%) in the y-axis and wavenumber (cm^{-1}) in the x-axis. A strong peak is shown at about 1000 cm^{-1}. Three small peaks at about 800 - 700 cm^{-1}. Three stronger peaks at about 500 - 400 cm^{-1}.

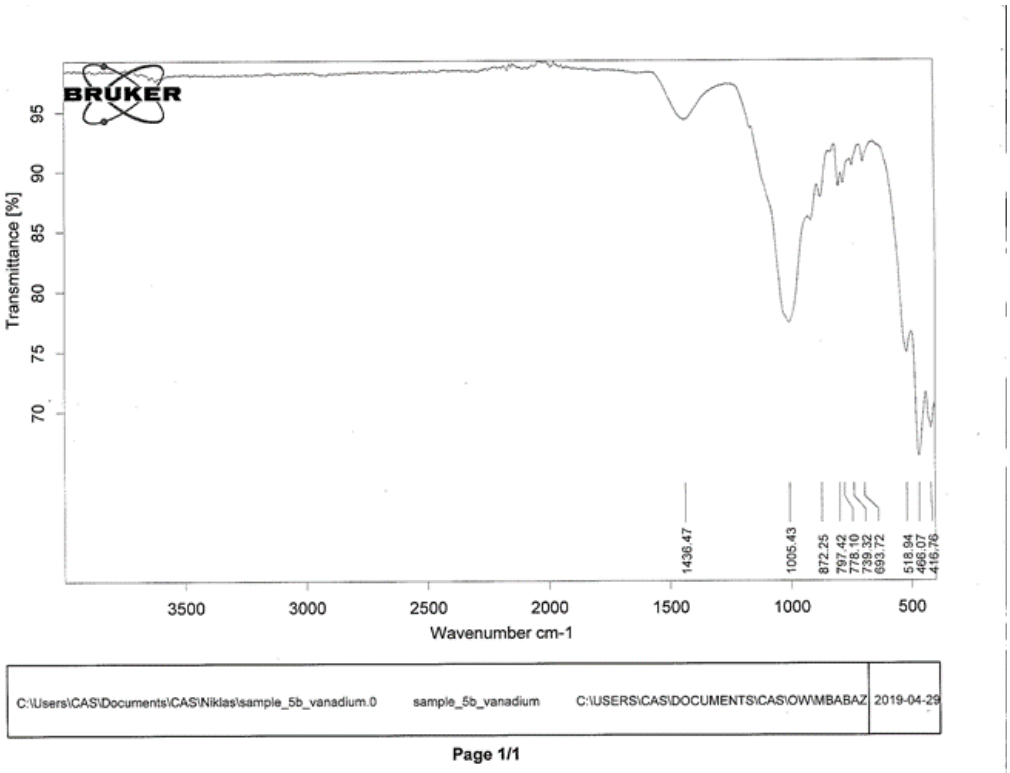

Fig 14. Spectrum of sample 5. Transmittance (%) in the y-axis and wavenumber (cm^{-1}) in the x-axis. A small broad peak at 1436 cm^{-1} which is not seen the in the other samples. A strong peak is shown at about 1000 cm^{-1}. Three small peaks at about 800 - 700 cm^{-1}. Four stronger peaks at about 500 - 400 cm^{-1}.

TOC-Analysis

Five samples were analyzed. The samples were chosen because of their variety in amount of vanadium and depth, their total carbon and organic carbon in percentage are presented in *table 11*. Three of the samples displayed a higher amount of organic carbon than total carbon.

The percentage of organic carbon has been multiplied by a factor of 100 to easier display a correlation with vanadium in *figure 15*. The graph show no correlation in the beginning, the three last values follow each other slightly.

Table 11: The samples analyzed, with the total carbon and organic carbon in percent and their vanadium content in ppm at depths in m.

Sample nr.	Total carbon (%)	Organic carbon (%)	Vanadium (ppm)	Depth (m)
4	8,6081	8,5394	997	20,07
10	8,7124	8,5995	791	17,34
21	11,2186	11,3481	278	12,95
40	13,6887	14,826	1010	4,23
55	12,3257	13,0113	588	0,62

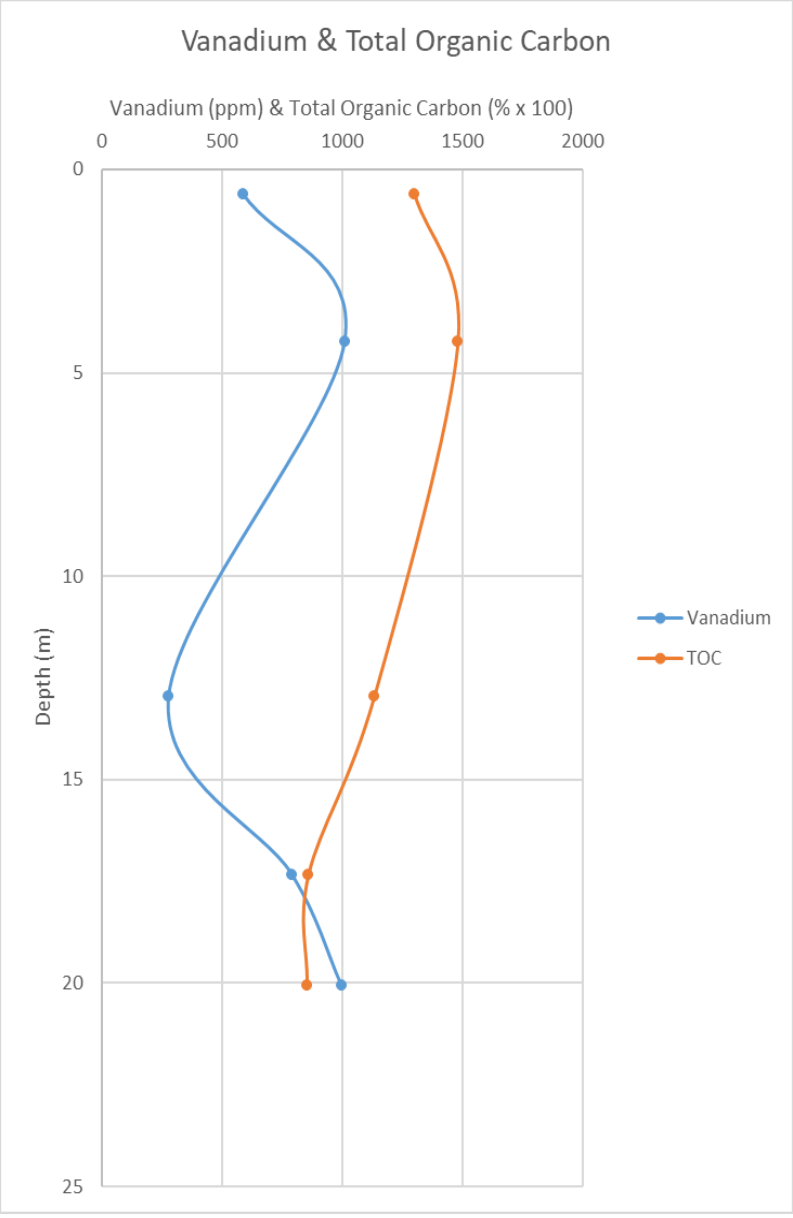

Fig. 15 Vanadium (ppm) and the total organic carbon in percent multiplied by a factor of 100 at different depths in the core section.

4 Discussion

The significance of the XRF results are mainly in how the elements vary in relation to depth to see where the drill is most enriched with respective trace element. If the composition throughout the drill core is presented in mean values, anomalies are included and may affect the value greatly. The mean values compared to the medians, in *table 1*, shows that Sn, Th, Bi, W, Co and P occurs anomalous. They are present at some points and not throughout the core. The values for P are highly uncertain due to error in calibration. Since the core was measured in closer intervals at 0,5 – 1,0 m depth, the mean value is slightly shifted. The shifted mean values and the presence of anomalous values favor the median as more representable values.

Since the median is a more representable value for the elements, these are preferred to compare with Clarke values. The trace elements of the alum shale drill core compared to the Clarke values of black shale were similar. The deviations show the difference in enrichment especially in U and Mo but also Ba, As, Pb, Cu and Ni. Of these Mo, As and Ni are known to be incorporated in pyrite, also U, Pb and V, but to a lesser extent, through different mechanisms.

The amount of vanadium, as seen in figure 3, increases towards the top, probably due to increased organic carbon. In the top-most section, a unexpected decrease of vanadium is seen.

As shown in *figure 10, 11 and 12* the signal of pyrite at 20,07 m, 12,95 m and 0,62 m was strong in the XRD spectra. This indicates a high abundance of pyrite. The strongest pyrite signal is seen at 12,95 m, *figure 11*. If compared to, *figure 9*, the highest peak of both Fe and S is at 12,95 m, matching the strongest pyrite signal.

If the strongest pyrite signal at 12,95 m is compared with the values of U and Mo at 12,95 m, in *figure 4 and 5*, are not higher than their mean or median values, in *table 1*. They are also not higher than the values of sample 55, at 0,62 m, where the third XRD measurement was made. There seem to be no correlation between the enrichment of pyrite in sample 21 and high abundance of U and Mo. It could be that the lower levels of pyrite is enough for all U to adsorb and Mo be incorporated, meaning that the concentration of U and Mo are the limiting factors respectively.

If the same comparison is made with V, it can be seen, in *table 1*, that V has a lower ppm at 12,95 m than its mean and median value. Pyrite incorporates V to a lesser extent, but not enough for a visible correlation.

The peak at 0,78 m which is found both in U, *figure 4* and Mo, *figure 5*, is not found in V, *figure 3*. There is also no correlation otherwise.

Ba has a sudden peak at 4,23 m, *figure 6*, which is also where the highest amount of V is located, no strong correlation was otherwise found.

The correlation of V and Ni can be seen in *figure 7*. They both bind to tetrapyrroles in the pore water of the sediment. This could be an indication of this pathway as the main process of vanadium accumulation. The deviation is at 1,02 m where the sample seem to contain a concentrated pocket of Ni.

The ratio of V / (Ni + V) can be used as a measurement of anoxia in the water. The value, in *figure 8*, is constantly between 0,6 – 0,8 with one exception of 0,43 at 1,02 m. The deviation in the ratio is a result of a discontinuation of correlation between V and Ni. The source of the deviating data point is found in a sudden peak of Ni at 1,02 m in *figure 7*. The sudden drop of the V / (Ni + V) ratio implies that there was a decline in anoxia, more oxygen was dissolved in the water, followed by an increase to the same fluctuating levels within the 0,6 – 0,8 ratio. Around1,02 m, at the topmost section, there is also a dip in the amount of V in the measurement, the less anoxic water may have hindered the reduction of V. Around this depth, the measurements were done with a decreased interval, increasing the probability of the decrease in vanadium to be statistically correct.

The x-ray diffraction spectra gave the highest signal for quartz, which may be expected due to the high level of Si as seen in *table 3*. The presence of O cannot be detected by XRF. Illite, which should be the main carrier of vanadium through exchange with Al, is shown at low signals in all spectra. Of the tabled data of illites three strongest peaks, only the two strongest are found in the spectra. The third at $2\theta = 24{,}30$ is not present in any of the spectra. This peak should have an intensity of 40% compared to the strongest illite peak. The low intensity of this third peak makes it harder to find among the other minerals. This indicates that the amount of illite in the three samples measured is low. No correlation is found if comparing the amount of V with illite intensities. Sample 21, at 12,95 m, has the greatest intensities of illite, with the highest peak at 54,12% but the lowest amount of V at 278 ppm. Sample 4, at 20,07 m, with 997 ppm V, has its greatest illite peak at 51,88 %. This indicates that vanadium is the limiting factor and not illite.

All major peaks were identified and no other vanadium bearing minerals were found. The low level of illite and lack of correlation with V, could also be an implication of another major phase for V, such as organic matter.

The XPS-spectra did not provide a signal strong enough to analyze vanadium. An alternative method should be used which can penetrate the samples deeper.

From the IR-spectra no match for vanadyl compounds were found. Due to the difficulty of identification in the fingerprint region, the presence of vanadyl still cannot be ruled out because of the great number of compounds and difficulty in identification.

The results of the TOC-analysis shows three values in which the amount of organic carbon is higher than the total carbon. This is probably the result of some error in the preparation for the combustion analysis. A probable cause of error was the decantation, there might

still have been particles suspended in the liquid after centrifugation.

Since there was a small difference between the organic carbon and total carbon a comparison with vanadium is still valid. A correlation is hard to see because of too few data point of organic carbon. It is plausible that a correlation would be found, with more data point, since vanadium is bound to organic matter in the sediment.

5 Conclusions

The drill core from Kinnekulle is more enriched in vanadium than the average black shale. The other elements which shows the most pronounced enrichment compared to average black shale values are barium, molybdenum, uranium, lead, copper and nickel.

The core has high amount of quartz and pyrite, but lower amount of illite. This could be an implication of the organic phase as a major carrier for vanadium.

The ratio of V / (Ni + V) indicated stable levels of anoxia until at 1,02 m, where there is a sudden decrease in anoxia.

The amount of vanadium increases towards the top but decreases at the top-most section. This decrease in vanadium could be due to the lower levels of anoxia.

6 Proposed further research

It would be of great interest to see if the paleontology change at the depth of 0,98 – 1,33 m, where the V / (Ni + V) ratio suggest a change in anoxia, compared to the rest of the core.

To determine the oxidation state of vanadium in the drill core, a method should be used that penetrates the samples deeper than XPS, which only analyze to about 1 nm of depth. A proposed method could be XANES, X-ray Absorption Near Edge Structure, which is not as sensitive but can determine the oxidation state.

Measuring the total organic carbon in all the samples would give a better understanding if there is a correlation with vanadium, and also with other trace elements.

7 Acknowledgements

First and foremost I would like to express my gratitude to my supervisors Mikael Calner at the Deparment of Geology and Ola Wendt at Department of Chemistry, and to Leif Johansson at the Department of Geology for guidance. All three have contributed with support, insights and made this project possible.

I would like to thank the Department of Geology for welcoming me and making it possible for me explore the field of geochemistry.

I would like to thank Martin Jarenmark at the Department of Geology for the idea for the project and introducing me to the department.

I would also like to thank:

Laura Folkers at the Department of Chemistry.

Niclas Johansson and the staff at SPECIES beamline, at MAX IV.

The members of Ola Wendt group, M. Seetharaman, A. Mousa and R. Mbabaz at the Department of Chemistry.

Karl Ljung at the Department of Geology.

Frans Lundberg at the Department of Geology.

8 References

Andersson, A., Dahlman, B., Gee, D. G. & Snäll, S., 1985: *The Scandinavian alum shales*. SGU ;, Uppsala :.

Breit, G. N. & Wanty, R. B., 1991: Vanadium accumulation in carbonaceous rocks: A review of geochemical controls during deposition and diagenesis. *Chemical Geology 91*, 83-97. doi: 10.1016/0009-2541(91)90083-4

Buchardt, B., Nielsen, A. T. & Schovsbo, N. H., 1997: *Alun skiferen i Skandinavien*. København : Dansk geologisk forening, 1997.

Chatterjee, A. K. 2001: 8 - X-Ray Diffraction. *In* V. S. Ramachandran & J. J. Beaudoin (eds.): *Handbook of Analytical Techniques in Concrete Science and Technology*, 275-332. William Andrew Publishing, Norwich, NY.

Crans, D. C. & Tracey, A. S. 1998: The Chemistry of Vanadium in Aqueous and Nonaqueous Solution. *In Vanadium Compounds*, 2-29. American Chemical Society,

Energy Storage Association, n.d.: Vanadium Redox (VRB) Flow Batteries. Retrieved 2019-05-03, from http://energystorage.org/energy-storage/technologies/vanadium-redox-vrb-flow-batteries.

George N. Breit, R. B. W., And Michele L. Tuttle, 1989: Metalliferous Black Shales and Related Ore Deposits. *In:* U. S. D. o. t. Interior (ed.) *Geochemi-*

cal Control on the Abundance of Vanadium in Black Shales and Other Carbonaceous Rocks. United States Working Group Meeting, International Geological Correlation Program Project 254, U.S. GEOLOGICAL SURVEY CIRCULAR 1058. 6-8 pp.

Housecroft, C. E. & Sharpe, A. G., 2018: *Inorganic chemistry*. Pearson, Harlow**.**

Kalnicky, D. J. & Singhvi, R., 2001: Field portable XRF analysis of environmental samples. *Journal of Hazardous Materials 83***,** 93-122. doi: https://doi.org/10.1016/S0304-3894(00)00330-7

Kelley, K. D., Scott, C. T., Polyak, D. E. & Kimball, B. E., 2017. Vanadium. Report 1802U, Reston, VA, 48 pp.

Ketris, M. P. & Yudovich, Y. E., 2009: Estimations of Clarkes for Carbonaceous biolithes: World averages for trace element contents in black shales and coals. *International Journal of Coal Geology 78***,** 135-148. doi: https://doi.org/10.1016/j.coal.2009.01.002

Lee, K. 1983: Vanadium in the aquatic ecosystem. *In*, 155-187,

Lerat, J. G., Sterpenich, J., Mosser-Ruck, R., Lorgeoux, C., Bihannic, I., Fialips, C. I., Schovsbo, N. H., Pironon, J. & Gaucher, É. C., 2018: Metals and radionuclides (MaR) in the Alum Shale of Denmark: Identification of MaR-bearing phases for the better management of hydraulic fracturing waters. *Journal of Natural Gas Science and Engineering 53***,** 139-152. doi: https://doi.org/10.1016/j.jngse.2018.02.015

Lewan, M. & Maynard, J., 1982: *Factors controlling enrichment of vanadium and nickel in the bitumen of organic sedimentary rocks*. 2547-2560 pp.

Micera, G., Erre, L. S. & Dallocchio, R., 1988: Metal complex formation on the surface of amorphous aluminium hydroxide. Part III. Copper (II) complexes of O-phospho-L-serine and O-phospho-L-tyrosine. *Colloids and Surfaces 32***,** 249-256. doi: https://doi.org/10.1016/0166-6622(88)80020-9

Morse, J. W. & Luther, G. W., 1999: Chemical influences on trace metal-sulfide interactions in anoxic sediments. *Geochimica Et Cosmochimica Acta 63***,** 3373-3378. doi: https://doi.org/10.1016/S0016-7037(99)00258-6

Qafoku, N. P., Kukkadapu, R. K., Mckinley, J. P., Arey, B. W., Kelly, S. D., Wang, C., Resch, C. T. & Long, P. E., 2009: Uranium in Framboidal Pyrite from a Naturally Bioreduced Alluvial Sediment. *Environmental Science & Technology 43***,** 8528-8534. doi: 10.1021/es9017333

Shieh, C.-S. & Duedall, I. W., 1988: Role of amorphous ferric oxyhydroxide in removal of anthropogenic vanadium from seawater. *Marine Chemistry 25***,** 121-139. doi: https://doi.org/10.1016/0304-4203(88)90060-6

Sternbeck, J., Sohlenius, G. & Hallberg, R. O., 2000: Sedimentary Trace Elements as Proxies to Depositional Changes Induced by a Holocene Fresh-Brackish Water Transition. *Aquatic Geochemistry 6***,** 325-345. doi: 10.1023/A:1009680714930

Thermofischer Scientific, n.d.: Niton™ XL3t GOLDD+ XRF Analyzer. Retrieved 2019-05-19, from https://www.thermofisher.com/order/catalog/product/XL3TGOLDDPLUS.

University of Oregon Chemistry Department, n.d.: Photoelectric Effect Computer Simulation PHET. Retrieved 2019-05-23, from https://chemdemos.uoregon.edu/demos/Photoelectric-Effect-Computer-Simulation-PHET.

Web Mineral, n.d.: Minerals Arranged by X-Ray Powder Diffraction. Retrieved 2019-05-17, from http://webmineral.com/MySQL/xray.php?ed1=4.43&minmax=2#.XN7Q78gzZaQ.

Wenger, L. M. & Baker, D. R., 1986: Variations in organic geochemistry of anoxic-oxic black shale-carbonate sequences in the Pennsylvanian of the

Midcontinent, U.S.A. *Organic Geochemistry 10*, 85-92. doi: https://doi.org/10.1016/0146-6380(86)90011-2

Ünsal, M., 1982: *The accumulation and transfer of vanadium within the food chain*. 139-141 pp.

Zhang, Y. B., Zhang, Q., Cai, Y., Wang, D. P. & Li, K. W., 2015: The occurrence state of vanadium in the black shale-hosted vanadium deposits in Shangling of Guangxi Province, China. *Acta Geochimica 34*, 484-497. doi: 10.1007/s11631-015-0060-8

LUNDS UNIVERSITET